

Dissipation-induced bound states as a two-level system

H. P. Zhang and Z. Song*

School of Physics, Nankai University, Tianjin 300071, China

Potential wells are employed to constrain quantum particles into forming discrete energy levels, acting as artificial few-level systems. In contrast, an anti-parity-time (\mathcal{PT}) symmetric system can have a single pair of real energy levels, while all the remaining levels are unstable due to the negative imaginary part of the energy. In this work, we investigate the formation of bound states in a tight-binding chain induced by a harmonic imaginary potential. Exact solutions show that the real parts of energy levels are equidistant, while the imaginary parts are semi-negative definite and equidistant. This allows for the formation of an effective two-level system. For a given initial state with a wide range of profiles, the evolved state always converges to a superposition of two stable eigenstates. In addition, these two states are orthogonal under the Dirac inner product and can be mutually switched by applying a π pulse of a linear field. Our finding provides an alternative method for fabricating quantum devices through dissipation.

I. INTRODUCTION

The bound state concept pervades various branches of physics, including optics and condensed matter. A bound state refers to a particle confined within a localized region by a real-valued potential, often due to interactions with other particles, within the framework of the Hartree-Fock approximation. Throughout the field of physics, phenomena that are stable or in equilibrium can be elucidated by the concept of bound states, which applies to both quantum and classical systems. Experimentally, bound states can be engineered by introducing artificial defects into photonic crystals. These defects, arranged in an array, form what are known as coupled-resonator optical waveguides (CROWs), which enable nearly lossless guidance and manipulation of wave packets, including their bending [1–11].

In contemporary physics, the presence of a complex potential is now permissible, as non-Hermitian quantum mechanics has become a versatile framework for developing functional devices that operate within the non-Hermitian domain. The fundamental mechanism underlying non-Hermitian systems with parity-time (\mathcal{PT}) symmetry hinges on the concept of an imaginary potential [12–23]. This concept has been both theoretically explored and experimentally realized [24–33], serving as an essential building block for constructing such systems.

A non-Hermitian Hamiltonian exhibits unique characteristics that set it apart from its Hermitian counterpart in three distinct aspects. (i) Asymmetry hopping term can result in skin effect, a typical bound state [34–38]. (ii) Adding a pseudo-Hermitian term to a non-Hermitian Hamiltonian consistently reduces the level spacing. Conversely, a nontrivial Hermitian perturbation invariably results in level repulsion. The phenomenon of shrinking level spacing is analogous to the impact of a real potential on a quantum system [39]. (iii) In a system with energy levels featuring semi-negative imaginary compo-

nents, only those eigenstates with real-valued energies are considered stable.

In this work, we explore the formation of two-level system through the mechanism associated with the characteristic mentioned as feature (iii) (see fig. 1). We investigate the formation of bound states in a tight-binding chain induced by a harmonic imaginary potential. It is an anti- \mathcal{PT} symmetric system. Unlike \mathcal{PT} -symmetry accompanied by real eigenvalues, an anti- \mathcal{PT} symmetric system can have a single pair of real energy levels, while all the remaining levels are unstable due to the negative imaginary part of the energy. The phenomenon of dissipation gives rise to bound states that can be effectively described as a two-level system. We consider a tight-binding chain induced by a harmonic imaginary potential to demonstrate this feature. Exact solutions show that the real parts of energy levels are equidistant, while the imaginary parts are semi-negative definite and equidistant. This allows for the formation of an effective two-level system. For a given initial state with a wide range of profiles, the evolved state always converges to a superposition of two stable eigenstates. We also find that these two states are orthogonal under the Dirac inner product, and thus a superposition state obeys the Dirac probability-preserving dynamics. Therefore, although the two-level system is engineered by non-Hermitian terms, it acts as a conditional Hermitian device. In addition, it is shown that two states can be mutually switched by applying a π pulse of a linear field. We demonstrate the conclusions by numerical simulations. Our finding provides an alternative method for fabricating quantum devices through dissipation.

This paper is organized as follows. In Sec. II, we introduce the non-Hermitian model and present approximate solutions for low energy levels. In Sec. III and IV, we show that two-level quantum states can be dynamically prepared and operated. Finally, our conclusion is given in Sec. V.

* songtc@nankai.edu.cn

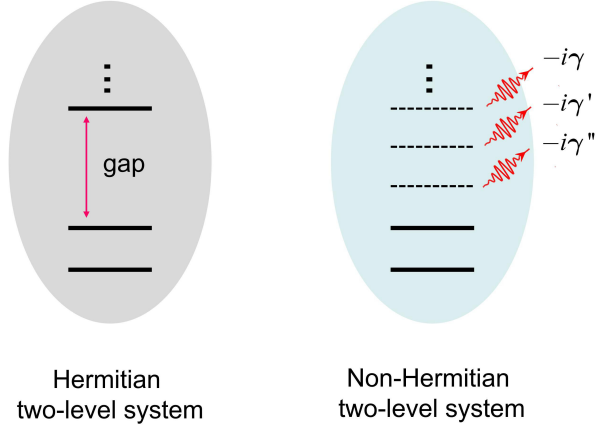


FIG. 1. Hermitian two-level system vs. non-Hermitian two-level system. (a) A Hermitian two-level system can be achieved in a many-body system when the gap between the first-excited state energy and the higher energy levels is sufficiently large. The time evolution preserves the Dirac probability for any initial state. (b) A non-Hermitian two-level system can be achieved in a many-body system when all the eigenstates decay with different rates $\gamma, \gamma', \gamma''$ and so on, except the two lower levels. In general, the Dirac probability for any initial state is periodic due to the biorthogonality of two-level states. Nevertheless, the proposed non-Hermitian two-level system can act as a Hermitian one.

II. HAMILTONIAN AND SYMMETRY

We start with the tight-binding model with the Hamiltonian

$$H = -J \sum_{l=-\infty}^{+\infty} (|l\rangle\langle l+1| + |l+1\rangle\langle l|) - iV \sum_{l=-\infty}^{+\infty} l^2 |l\rangle\langle l| + i\omega, \quad (1)$$

where $|l\rangle$ denotes a site state describing the Wannier state localized on the l th period of the potential. Here, $-J$ is the tunneling strength, and V is the strength of the harmonic potential. The system is schematically illustrated in fig. 2(a). In previous work, it has been shown that the lower energy levels are equidistant when the system is Hermitian by taking $V \rightarrow iV$ [40, 41]. In this work, we take $J, V > 0$, and constant $\omega = \sqrt{JV}/2$. We note that the Hamiltonian has anti- \mathcal{PT} symmetry, satisfying

$$\mathcal{PT}H(\mathcal{PT})^{-1} = -H, \quad (2)$$

where the linear operator \mathcal{P} and antilinear operator \mathcal{T} are defined as

$$\mathcal{P}|l\rangle = (-1)^l |l\rangle, \mathcal{T}i\mathcal{T}^{-1} = -i. \quad (3)$$

The eigenstate $|\psi_m\rangle$, satisfying the Schrodinger equation

$$H|\psi_m\rangle = E_m|\psi_m\rangle, \quad (4)$$

can be written in the form

$$|\psi_m\rangle = \sum_l \psi_m(l) |l\rangle. \quad (5)$$

According to the non-Hermitian quantum mechanics [42], iH is a pseudo-Hermitian operator, and then iE_m can be real or come in complex conjugate pairs.

Specifically, we expect the solution for the wave function $\psi_m(l)$ to be connected to a continuous function, $\psi_m(x)$. In the following, we aim to obtain the approximate expression of the function $\psi_m(x)$, under certain conditions. The Schrodinger equation (4) shows that function $\psi_m(l)$ can be determined by the equation

$$\psi_m(l+1) + \psi_m(l-1) = \frac{i\omega - E_m - iVl^2}{J} \psi_m(l). \quad (6)$$

We propose two types of functions $\psi_m^\pm(l)$ as the Bethe ansatz wave function, which are defined as

$$\psi_m^+(l) = N_m \exp(-\frac{\alpha^2 l^2}{2}) H_m(\alpha l), \quad (7)$$

and

$$\psi_m^-(l) = (-1)^l [\psi_m^+(l)]^*, \quad (8)$$

with coefficients $\alpha = e^{-i\pi/8}(V/J)^{1/4}$ and $(N_m)^{-2} = \int_{-\infty}^{+\infty} H_m(\alpha x) H_m(\alpha^* x) \times e^{-\text{Re}\alpha^2 x^2} dx$. Obviously, $\psi_m^\pm(x)$ are eigen functions of quantum oscillator system, satisfying the differential equation

$$\left[\frac{d^2}{dx^2} - \alpha^4 x^2 + \alpha^2(2m+1) \right] \psi_m^\pm = 0. \quad (9)$$

with $m = 0, 1, 2, \dots$. As known that function $\psi_m^+(x)$ is smooth and slowly varying for small m and α (or $V \ll J$), where $H_m(\alpha x)$ is the Hermite polynomials. This allows the approximation

$$\psi_m^+(x+1) + \psi_m^+(x-1) \approx 2\psi_m^+(x) + \frac{d^2}{dx^2} \psi_m^+(x), \quad (10)$$

resulting in the eigen energy levels

$$E_m^+ = [(2m+1)\omega - 2J] - i2m\omega, \quad (11)$$

in association with Eqs. (6) and (9). Similarly, we have

$$E_m^- = [2J - (2m+1)\omega] - i2m\omega. \quad (12)$$

It accords with the prediction with the relations

$$\mathcal{PT}|\psi_m^+\rangle = |\psi_m^-\rangle, \quad (13)$$

and

$$(iE_m^+) = (iE_m^-)^*, \quad (14)$$

i.e., the real parts of the levels are paired with opposite signs. The additional feature of the energy levels is that their imaginary parts are semi-negative finite and equally distant, which is schematically illustrated in fig. 2(b).

Remarkably, there are only two eigenstates have real energy, with wave function and eigen energy

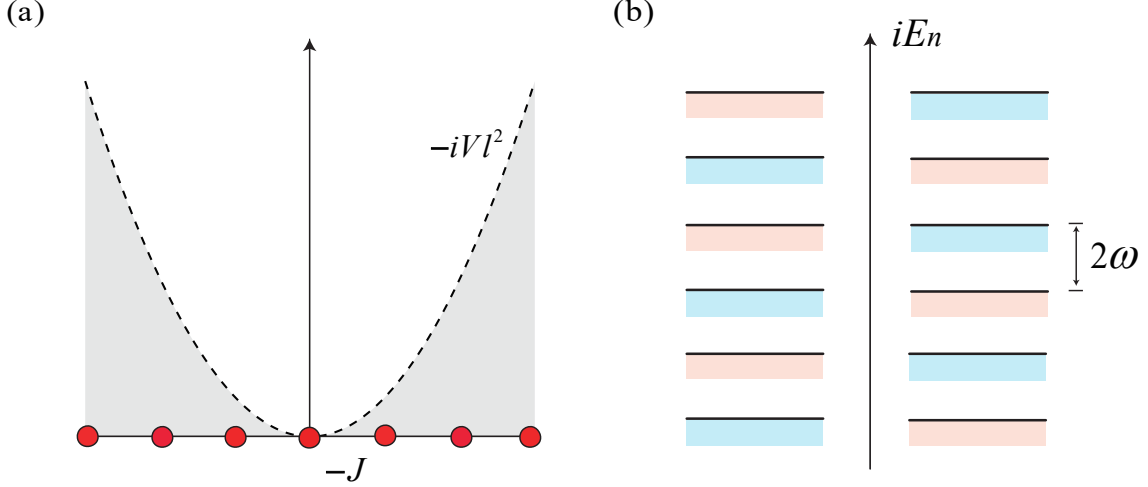


FIG. 2. (a) Schematic illustrations of the Hamiltonian in Eq. (1), which represents a tight-binding chain with adjacent hopping strengths is $-J$ and on-site imaginary potential $-iVl^2$ (a constant $i\omega$ is omitted). The anti- \mathcal{PT} symmetry of the system ensures the following characteristics for the energy level structure. (b) Energy level structure diagrams for Hamiltonian of (a). E_n stands for eigenenergy of the Hamiltonian in Eq. (1). The solid line represents the real part of iE_n with isoenergetic distance 2ω . The red and blue blocks represent the positive imaginary part and negative imaginary part of iE_n , respectively. It can be seen that iE_n is composed of conjugate pair energy levels due to the pseudo Hermiticity of the Hamiltonian iH .

$$\psi_0^\pm(l) = (\pm 1)^l N_0 e^{-\omega l^2/(2J)} e^{\pm i\omega l^2/(2J)}, \quad (15)$$

$$E_0^\pm = \mp(2J - \omega), \quad (16)$$

where the normalization factor $N_0 = [V/(2J\pi^2)]^{1/8}$. All the rest eigenstates decay as time increases. In this sense, such a system only supports two stable eigenstates, the ground state

$$|g\rangle = |\psi_0^+\rangle, \quad (17)$$

and the excited state

$$|e\rangle = |\psi_0^-\rangle. \quad (18)$$

In general, two different eigenstates are biorthogonal for non-Hermitian system, which satisfy the relationship, i.e., $\langle \varphi_n^\sigma | \psi_m^{\sigma'} \rangle = \delta_{nm} \delta_{\sigma\sigma'}$ [43]. It accords with the fact that we have

$$\langle \varphi_0^\pm | \psi_0^\mp \rangle = \sum_{l=-\infty}^{+\infty} (-1)^l N_0^2 e^{-\omega l^2/J} = 0, \quad (19)$$

in the limit $\omega/J \rightarrow 0$ (or $\alpha \rightarrow 0$), where $|\varphi_0^\pm\rangle$ satisfies

$$H^* |\varphi_0^\pm\rangle = (E_0^\pm)^* |\varphi_0^\pm\rangle. \quad (20)$$

Meanwhile, we also have

$$\langle e | g \rangle = \sum_{l=-\infty}^{+\infty} (-1)^l N_0^2 e^{-(1-i)\omega l^2/J} = 0, \quad (21)$$

in such a limit, which indicates that the Dirac orthogonality still holds. Therefore, such a non-Hermitian system can be regarded as a Hermitian two-level system.

III. TWO-LEVEL DYNAMICS

In quantum physics, two-level atoms are simple yet rich quantum systems that are fundamental to our understanding of quantum mechanics and are essential for the development of quantum technologies. The ability to control and manipulate these systems is at the heart of many advances in quantum science.

In a Hermitian system, an effective two-level system can be formed when the ground state and the excited state have relative large energy gap from the high excited states. In contrast, a distinguishing characteristic of the non-Hermitian two-level system is that the all other eigenstates are unstable in dynamics or short lived (see fig. 1). This enables the system to exhibit the following dynamical behaviors.

We start with the time evolution for an arbitrary initial state $|\Phi(0)\rangle$, which can always be expressed as the form

$$|\Phi(0)\rangle = \sum_n (c_n^+ |\psi_n^+\rangle + c_n^- |\psi_n^-\rangle), \quad (22)$$

in the framework of the above approximation approach. Thus, the time evolved state is

$$|\Phi(t)\rangle = \sum_{n,\pm} c_n^\pm e^{-iE_n^\pm t} |\psi_n^\pm\rangle, \quad (23)$$

which tends to

$$|\Phi(t)\rangle = c_0^+ e^{-iE_0^+ t} |g\rangle + c_0^- e^{-iE_0^- t} |e\rangle, \quad (24)$$

after a long time.

Specifically, for an initial state $|\Phi(0)\rangle$ with the wave function $\langle l | \Phi(0) \rangle$ varying slowly as l changes, we have

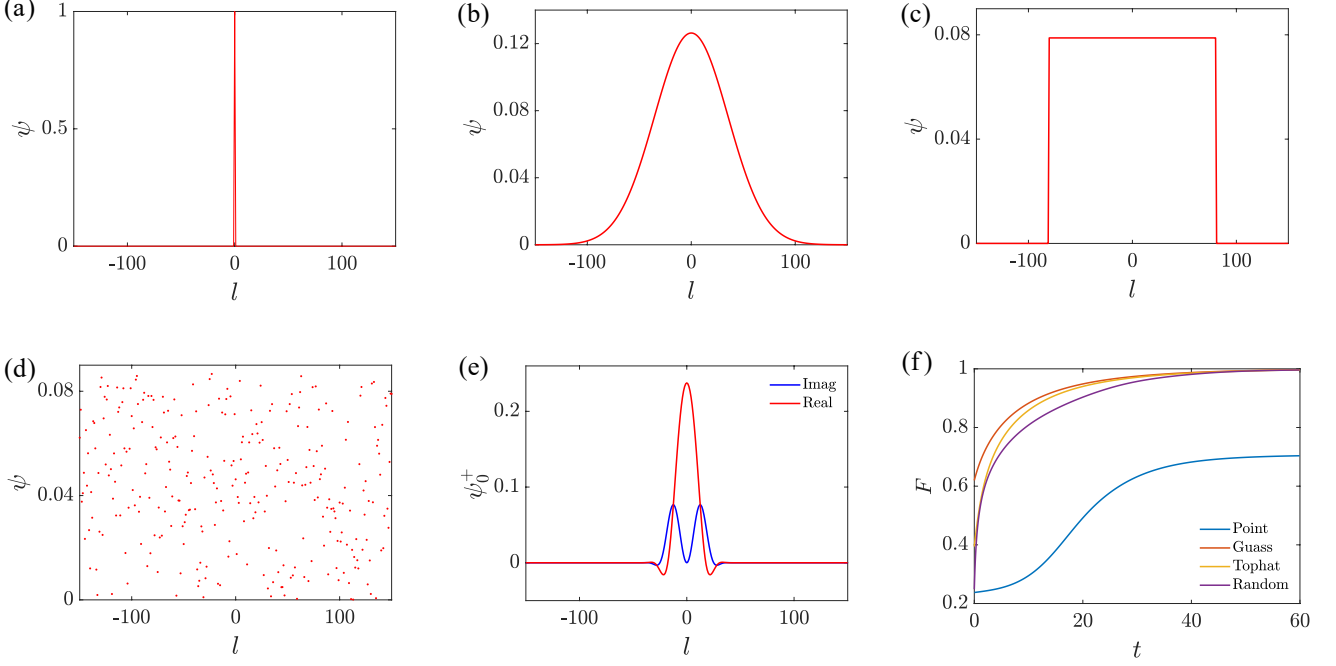


FIG. 3. Plots of the profiles of initial states and the fidelities of the corresponding evolved states to the given target states. (a-d) Initial states feature several typical amplitude distributions: point (delta function), Gaussian, tophat, and random (stochastic) functions. (e) is the plot of ground state of the non-Hermitian two-level system as the target state. (f) is the plot of fidelity $F(t)$ defined in Eq. (25). We can see that the final states for (b), (c) and (d) are the same, the ground state, while the superposition of ground state and excited state for (a). The unit of time is $1/J$ and the system parameters are $J = 1$, $V = 2 \times 10^{-4}$, and $\omega = 10^{-2}$.

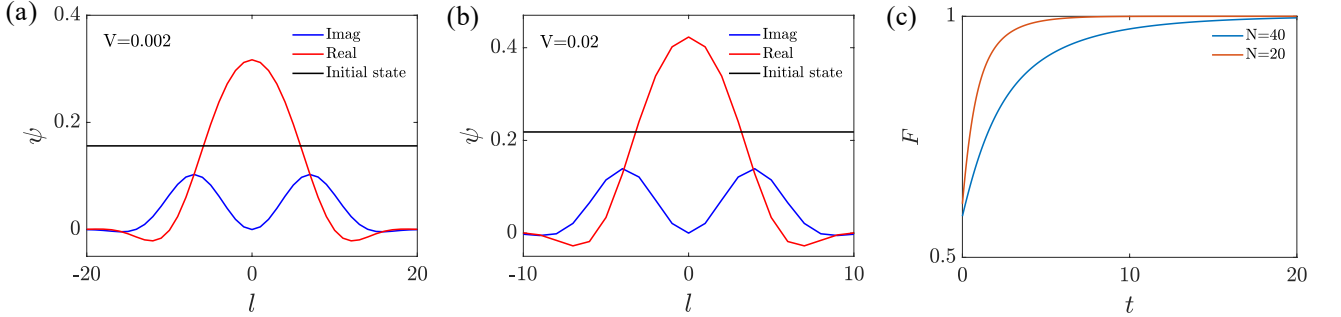


FIG. 4. Plots of the profiles of ground states (target states) under different system parameters and the fidelities of the corresponding evolved states to the given target states. The system parameters are (a) $N = 40$, $V = 0.002$ and $J = 1$; (b) $N = 20$, $V = 0.02$ and $J = 1$. The red line and blue line represent the real and imaginary parts of the ground state, respectively, while the black line indicates the initial state. The plot of fidelity $F(t)$ in (c) defined in Eq. 25 for (a) and (b) is obtained by numerical simulation. It can be observed that increasing V significantly shortens the time required for the fidelity to reach 1.

$c_0^- = 0$ and $|\Phi(\infty)\rangle \propto |g\rangle$. Then, the ground state $|g\rangle$ can be dynamically generated from a variety of initial states. Note that the analytical expressions of $|g\rangle$ and $|e\rangle$ from $|\psi_0^\pm\rangle$ are approximate. In practice, such two states can be obtained from numerical simulations. To verify and demonstrate the above results, numerical simulations of the dynamic process are performed using a uniform mesh for the time discretization.

We calculate the fidelity

$$F(t) = |\langle g | e^{-iHt} |\Phi(0)\rangle| / |e^{-iHt} |\Phi(0)\rangle|^2, \quad (25)$$

to measure the distance between the evolved state and the target state. We plot several typical initial states $\langle l | \Phi(0) \rangle$ and $F(t)$ in fig. 3. These numerical results are consistent with our previous analysis, which showed that the evolved states converge to the state $|g\rangle$ for several selected initial states. Therefore, we conclude that a harmonic imaginary potential can support the stable bound

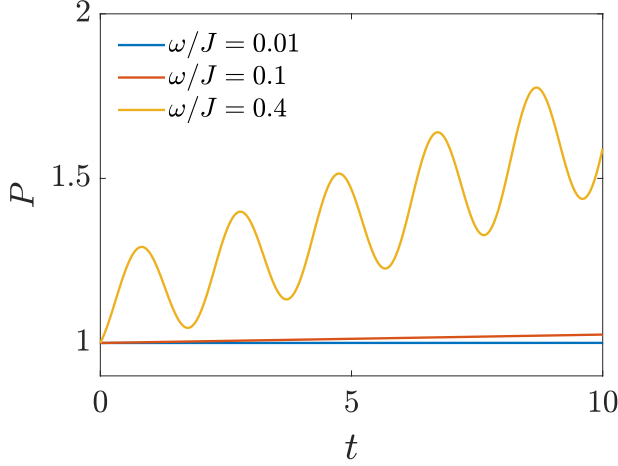


FIG. 5. Plots of $P(t)$ defined in Eq. (26) for several different ω/J . (a)(b)(c) respectively correspond to $\omega/J = 0.01, 0.1, 0.4$. It can be seen that when ω/J is small (< 0.1), the Dirac probability is almost conserved, which indicates that our approximation is appropriate. The unit of time is $1/J$ and the system parameters are $J = 1$.

state $|g\rangle$, which can also be prepared dynamically. We also investigate the small size systems by numerical simulation. We plot the profiles of ground states and $F(t)$ of evolving from a uniform initial state in fig. 4. It indicates that a small system size requires a small width of the wavefunction profile, which requires a large V (or ω), resulting in faster convergence. The small size and the faster convergence of the fidelity make the scheme experimentally feasible.

In general, the dynamics of a non-Hermitian two-level system are not Dirac probability-preserving. However, as mentioned above, we have $\langle e|g\rangle = 0$ in the limit $\omega/J \rightarrow 0$ (or $\alpha \rightarrow 0$). This indicates that a superposition state obeys the Dirac probability-preserving dynamics. We demonstrate this point by computing the probability

$$P(t) = |\langle \Phi(t) | \Phi(t) \rangle|^2 \quad (26)$$

for initial state

$$|\Phi(0)\rangle = \frac{1}{\sqrt{2}} (|g\rangle + |e\rangle), \quad (27)$$

where $|g\rangle$ and $|e\rangle$ are obtained by the numerical simulation for the systems with different values of ω/J . The plots of the $P(t)$ function in fig. 5 conform to the theoretical predictions we established.

IV. TRANSITION BETWEEN TWO LEVELS

In parallel, one can dynamically generate the excited state $|e\rangle$ from initial states with $c_0^+ = 0$. In this section, we focus on a scheme designed to facilitate the transition between the two states $|g\rangle$ and $|e\rangle$. Based on the

above analysis, a possible clue is provided by the relation $\mathcal{PT}|g\rangle = |e\rangle$. We start with the dynamic realization of operator \mathcal{P} .

We consider to realize the action of operator \mathcal{P} by the time evolution under a quenching Hamiltonian

$$H_{\text{quen}} = H + H_p(t), \quad (28)$$

where

$$H_p(t) = \mu(t) \sum_{l=-\infty}^{+\infty} l|l\rangle\langle l|, \quad (29)$$

describes the action of an extra time-dependent uniform field. Here the coefficient is defined as

$$\mu(t) = \begin{cases} \frac{\pi}{\Delta}, & 0 < t < \Delta \\ 0, & \text{otherwise} \end{cases}, \quad (30)$$

with which $H_p(t)$ acts as a π pulse. In general, the time evolution of a given initial state is governed by the time propagator

$$U(t) = \exp \left[-i \int_0^t H_{\text{quen}} dt \right]. \quad (31)$$

Under the condition $\pi/\Delta \gg 1$, we can have

$$\begin{aligned} U(t) &\approx \exp \left[-i \int_0^t H dt \right] \exp \left[-i \int_0^\Delta H_p(t) dt \right] \\ &= \exp \left[-i \int_0^t H dt \right] \prod_{l=-\infty}^{+\infty} \exp(-i\pi l) |l\rangle\langle l| \\ &= \exp \left[-i \int_0^t H dt \right] \mathcal{P}. \end{aligned} \quad (32)$$

It indicates that the time evolution of the initial state $|g\rangle$ is

$$U(t)|g\rangle = \exp \left[-i \int_0^t H dt \right] |e\rangle^*, \quad (33)$$

which tends to $|e\rangle$ after a long time. Inversely, we can also realize the operation

$$U(t)|e\rangle \rightarrow |g\rangle. \quad (34)$$

To verify this result, we perform numerical simulation for such a quenching process for two different initial states $|\Phi(0)\rangle = |g\rangle$ and $|e\rangle$, which are obtained by exact diagonalization of the pre-quench Hamiltonian H . We compute the two fidelities

$$F_g(t) = |\langle g | e^{-iHt} | g \rangle / |e^{-iHt} | g \rangle|^2, \quad (35)$$

$$F_e(t) = |\langle e | e^{-iHt} | g \rangle / |e^{-iHt} | g \rangle|^2, \quad (36)$$

to evaluate the efficiency of the scheme. It is expected that the fidelities obey $F_g(\infty) = 0$ and $F_e(\infty) = 1$ (or $F_e(\infty) = 0$ and $F_g(\infty) = 1$). The numerical results are presented in fig. 6(b), which are in accord with our analysis. Here the form of $\mu(t)$ is the simplest one for a π pulse. Other types of $\mu(t)$ could also have the same effect.

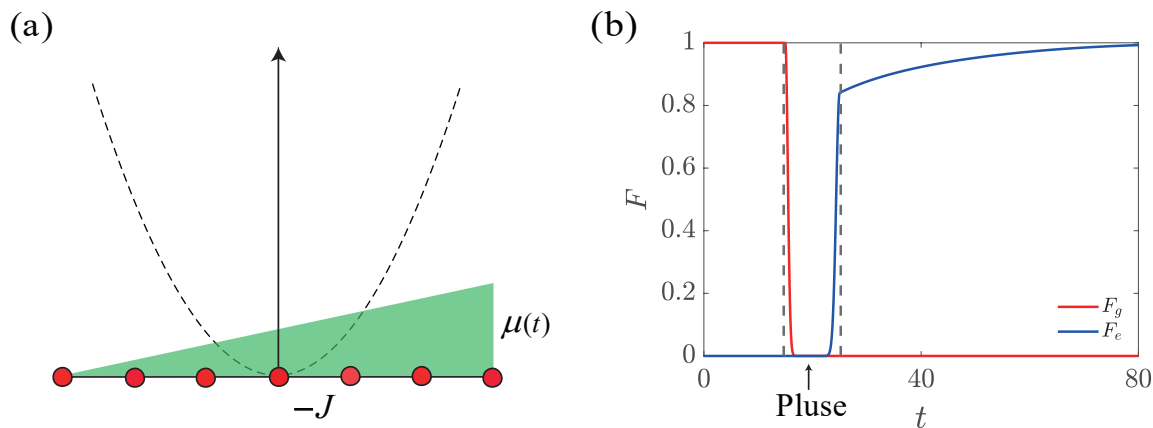


FIG. 6. (a) Schematic illustrations of the Hamiltonian in Eq. (28), which represents adding the time varying skew potential pulse $\mu(t)$ on the basis of the Hamiltonian in Eq. (1). (b) The plot of $F_g(t)$ and $F_e(t)$ defined in Eqs. (35) and (36) for initial state $|g\rangle$. For the case with initial state $|e\rangle$, an almost same figure is obtained by switching $F_g(t)$ with $F_e(t)$. It can be seen that the conversion between the ground state and the excited state can be realized by applying π pulse. The unit of time is $1/J$ and the system parameters are $J = 1$, $V = 2 \times 10^{-4}$, and $\omega = 10^{-2}$.

V. CONCLUSION AND DISCUSSION

In summary, we have studied the formation of two-level bound states induced by imaginary potential in a Hermitian tight-binding system. We have shown that the real parts of energy levels are equidistant, while the imaginary parts are semi-negative definite and equidistant. This allows for the formation of an effective two-level system. The existence of bound states in a system with an imaginary potential is fundamentally due to the fact that the corresponding Hermitian system has a discrete spatial coordinates, which arises from the presence of a periodic real potential. The similar phenomenon occurs in another non-Hermitian system. It has been shown in Ref. [44] that bound states can form in a tight-binding chain in the presence of a linear imaginary potential. This allows

for the formation of an effective two-level system. In contrast to a Hermitian two-level system, a non-Hermitian system can have a single pair of real energy levels, while the remaining levels are unstable due to their negative imaginary components. This feature enables the dynamic preparation and operation of two-level quantum states. Our findings reveal that the phenomenon of dissipation gives rise to bound states that can effectively be described as a two-level system.

ACKNOWLEDGMENTS

This work was supported by National Natural Science Foundation of China (under Grant No. 12374461).

-
- [1] S.G. Johnson, A. Mekis, S. Fan, and J.D. Joannopoulos, "Molding the flow of light," *Computing in Science and Engineering* **3**, 38–47 (2001).
 - [2] Sajeed John, "Strong localization of photons in certain disordered dielectric superlattices," *Physical Review Letters* **58**, 2486–2489 (1987).
 - [3] Eli Yablonovitch, "Inhibited Spontaneous Emission in Solid-State Physics and Electronics," *Physical Review Letters* **58**, 2059–2062 (1987).
 - [4] Maksim Skorobogatiy, Guillaume Begin, and Anne Talneau, "Statistical analysis of geometrical imperfections from the images of 2d photonic crystals," *Optics Express* **13**, 12487 (2005).
 - [5] R. J. P. Engelen, D. Mori, T. Baba, and L. Kuipers, "Two Regimes of Slow-Light Losses Revealed by Adiabatic Reduction of Group Velocity," *Physical Review Letters* **101**, 103901 (2008).
 - [6] S. Hughes, L. Ramunno, Jeff F. Young, and J. E. Sipe, "Extrinsic Optical Scattering Loss in Photonic Crystal Waveguides: Role of Fabrication Disorder and Photon Group Velocity," *Physical Review Letters* **94**, 033903 (2005).
 - [7] E. Kuramochi, M. Notomi, S. Hughes, A. Shinya, T. Watanabe, and L. Ramunno, "Disorder-induced scattering loss of line-defect waveguides in photonic crystal slabs," *Physical Review B* **72**, 161318 (2005).
 - [8] N. Le Thomas, V. Zabelin, R. Houdré, M. V. Kotlyar, and T. F. Krauss, "Influence of residual disorder on the anticrossing of Bloch modes probed in \mathbf{k} space," *Physical Review B* **78**, 125301 (2008).
 - [9] S. Mazoyer, J. P. Hugonin, and P. Lalanne, "Disorder-Induced Multiple Scattering in Photonic-Crystal Waveguides," *Physical Review Letters* **103**, 063903 (2009).
 - [10] S. Mazoyer, P. Lalanne, J.C. Rodier, J.P. Hugonin, M. Spasenović, L. Kuipers, D.M. Beggs, and T.F.

- Krauss, “Statistical fluctuations of transmission in slow light photonic-crystal waveguides,” *Optics Express* **18**, 14654 (2010).
- [11] Liam O’Faolain, Thomas P. White, David O’Brien, Xiadong Yuan, Michael D. Settle, and Thomas F. Krauss, “Dependence of extrinsic loss on group velocity in photonic crystal waveguides,” *Optics Express* **15**, 13129 (2007).
- [12] Carl M. Bender and Stefan Boettcher, “Real Spectra in Non-Hermitian Hamiltonians Having \mathcal{PT} Symmetry,” *Physical Review Letters* **80**, 5243–5246 (1998).
- [13] Patrick Dorey, Clare Dunning, and Roberto Tateo, “Spectral equivalences, bethe ansatz equations, and reality properties in \mathcal{PT} -symmetric quantum mechanics,” *Journal of Physics A: Mathematical and General* **34**, 5679–5704 (2001).
- [14] Ali Mostafazadeh, “Pseudo-Hermiticity versus \mathcal{PT} symmetry: the necessary condition for the reality of the spectrum of a non-Hermitian Hamiltonian,” *Journal of Mathematical Physics* **43**, 205–214 (2002).
- [15] Miloslav Znojil, “ \mathcal{PT} -symmetric harmonic oscillators,” *Physics Letters A* **259**, 220–223 (1999).
- [16] H F Jones, “On pseudo-Hermitian Hamiltonians and their Hermitian counterparts,” *Journal of Physics A: Mathematical and General* **38**, 1741–1746 (2005).
- [17] R. El-Ganainy, K. G. Makris, D. N. Christodoulides, and Ziad H. Musslimani, “Theory of coupled optical \mathcal{PT} -symmetric structures,” *Optics Letters* **32**, 2632 (2007).
- [18] Z. H. Musslimani, K. G. Makris, R. El-Ganainy, and D. N. Christodoulides, “Optical Solitons in \mathcal{PT} Periodic Potentials,” *Physical Review Letters* **100**, 030402 (2008).
- [19] K. G. Makris, R. El-Ganainy, D. N. Christodoulides, and Z. H. Musslimani, “Beam Dynamics in \mathcal{PT} Symmetric Optical Lattices,” *Physical Review Letters* **100**, 103904 (2008).
- [20] Yogesh N. Joglekar, Derek Scott, Mark Babbey, and Avadh Saxena, “Robust and fragile \mathcal{PT} -symmetric phases in a tight-binding chain,” *Physical Review A* **82**, 030103 (2010).
- [21] Derek D. Scott and Yogesh N. Joglekar, “Degrees and signatures of broken \mathcal{PT} symmetry in nonuniform lattices,” *Physical Review A* **83**, 050102 (2011).
- [22] Y. D. Chong, Li Ge, Hui Cao, and A. D. Stone, “Coherent Perfect Absorbers: Time-Reversed Lasers,” *Physical Review Letters* **105**, 053901 (2010).
- [23] Hui Jing, S.K. Özdemir, Xin-You Lü, Jing Zhang, Lan Yang, and Franco Nori, “ \mathcal{PT} -Symmetric Phonon Laser,” *Physical Review Letters* **113**, 053604 (2014).
- [24] A. Guo, G. J. Salamo, D. Duchsne, R. Morandotti, M. Volatier-Ravat, V. Aimez, G. A. Siviloglou, and D. N. Christodoulides, “Observation of \mathcal{PT} -Symmetry Breaking in Complex Optical Potentials,” *Physical Review Letters* **103**, 093902 (2009).
- [25] Christian E. Rüter, Konstantinos G. Makris, Ramy El-Ganainy, Demetrios N. Christodoulides, Mordechai Segev, and Detlef Kip, “Observation of parity–time symmetry in optics,” *Nature Physics* **6**, 192–195 (2010).
- [26] Wenjie Wan, Yidong Chong, Li Ge, Heeso Noh, A. Douglas Stone, and Hui Cao, “Time-Reversed Lasing and Interferometric Control of Absorption,” *Science* **331**, 889–892 (2011).
- [27] Yong Sun, Wei Tan, Hong-qiang Li, Jensen Li, and Hong Chen, “Experimental Demonstration of a Coherent Perfect Absorber with \mathcal{PT} Phase Transition,” *Physical Review Letters* **112**, 143903 (2014).
- [28] Liang Feng, Ye-Long Xu, William S. Fegadolli, Ming-Hui Lu, José E. B. Oliveira, Vilson R. Almeida, Yan-Feng Chen, and Axel Scherer, “Experimental demonstration of a unidirectional reflectionless parity-time metamaterial at optical frequencies,” *Nature Materials* **12**, 108–113 (2012).
- [29] Bo Peng, Şahin Kaya Özdemir, Fuchuan Lei, Faraz Monifi, Mariagiovanna Gianfreda, Gui Lu Long, Shan-hui Fan, Franco Nori, Carl M. Bender, and Lan Yang, “Parity–time-symmetric whispering-gallery microcavities,” *Nature Physics* **10**, 394–398 (2014).
- [30] Long Chang, Xiaoshun Jiang, Shiyue Hua, Chao Yang, Jianming Wen, Liang Jiang, Guanyu Li, Guanzhong Wang, and Min Xiao, “Parity–time symmetry and variable optical isolation in active–passive-coupled microresonators,” *Nature Photonics* **8**, 524–529 (2014).
- [31] Liang Feng, Zi Jing Wong, Ren-Min Ma, Yuan Wang, and Xiang Zhang, “Single-mode laser by parity-time symmetry breaking,” *Science* **346**, 972–975 (2014).
- [32] Hossein Hodaei, Mohammad-Ali Miri, Matthias Heinrich, Demetrios N. Christodoulides, and Mercedeh Khajavikhan, “Parity-time–symmetric microring lasers,” *Science* **346**, 975–978 (2014).
- [33] Martin Wimmer, Alois Regensburger, Mohammad-Ali Miri, Christoph Bersch, Demetrios N. Christodoulides, and Ulf Peschel, “Observation of optical solitons in \mathcal{PT} -symmetric lattices,” *Nature Communications* **6** (2015), 10.1038/ncomms8782.
- [34] X.Z. Zhang and Z. Song, “Momentum-independent reflectionless transmission in the non-Hermitian time-reversal symmetric system,” *Annals of Physics* **339**, 109–121 (2013).
- [35] Flore K. Kunst, Elisabet Edvardsson, Jan Carl Budich, and Emil J. Bergholtz, “Biorthogonal Bulk-Boundary Correspondence in Non-Hermitian Systems,” *Physical Review Letters* **121**, 026808 (2018).
- [36] Shunyu Yao and Zhong Wang, “Edge States and Topological Invariants of Non-Hermitian Systems,” *Physical Review Letters* **121**, 086803 (2018).
- [37] Zongping Gong, Yuto Ashida, Kohei Kawabata, Kazuaki Takasan, Sho Higashikawa, and Masahito Ueda, “Topological Phases of Non-Hermitian Systems,” *Physical Review X* **8**, 031079 (2018).
- [38] L. Jin and Z. Song, “Bulk-boundary correspondence in a non-Hermitian system in one dimension with chiral inversion symmetry,” *Physical Review B* **99**, 081103 (2019).
- [39] K. L. Zhang, P. Wang, and Z. Song, “Exceptional-point-induced lasing dynamics in a non-Hermitian Su-Schrieffer-Heeger model,” *Physical Review A* **99**, 042111 (2019).
- [40] Tao Shi, Ying Li, Zhi Song, and Chang-Pu Sun, “Quantum-state transfer via the ferromagnetic chain in a spatially modulated field,” *Physical Review A* **71**, 032309 (2005).
- [41] Shi Tao, Chen Bing, and Song Zhi, “On Harmonic Approximation for Large Josephson Junction Coupling Charge Qubits,” *Communications in Theoretical Physics* **43**, 795–798 (2005).
- [42] F.G. Scholtz, H.B. Geyer, and F.J.W. Hahne, “Quasi-Hermitian operators in quantum mechanics and the variational principle,” *Annals of Physics* **213**, 74–101 (1992).

- [43] Dorje C Brody, “Biorthogonal quantum mechanics,” [Journal of Physics A: Mathematical and Theoretical](#) **47**, 035305 (2013). [arXiv:2401.13286 \[quant-ph\]](#).
- [44] H. P. Zhang, K. L. Zhang, and Z. Song, “Dynamics of non-Hermitian Floquet Wannier-Stark system,” (2024),